ELSEVIER

Biochimica et Biophysica Acta 1326 (1997) 257–264

BIOCHIMICA ET BIOPHYSICA ACTA
BBA

The molecular area characteristics of the HIV-1 gp41-fusion peptide at the air/water interface. Effect of pH

Susanne E. Taylor, Gerhard Schwarz *

Department of Biophysical Chemistry, Biocenter of the University, Klingelbergstr. 70, CH 4056 Basel, Switzerland

Received 17 December 1996; accepted 4 February 1997

Abstract

The putative fusion peptide of HIV-1 is a highly surface active substance. Relevant measurements with the Langmuir monolayer technique have been carried out for a broad range of the pH in the aqueous subphase. The data are processed towards a quantitative analysis of the partitioning equilibrium between the interfacial and aqueous moieties. Our results reveal a pronounced decrease of the surface area per peptide molecule upon monolayer compression. This phenomenon could be interpreted in terms of an orientational transition experienced by an α-helical peptide structure. The area requirements at any fixed lateral pressure pass through a distinct minimum at a pH of 5.5 (± 0.5). Such an apparent isoelectric point was confirmed by isoelectric focusing of peptide aggregates. Accordingly a drastic drop of the pK-values of the two basic amino acid residues in comparison with an aqueous medium is indicated. It can be readily explained based on an inherent decrease of the effective dielectric constant. The observed low pH in favor of an enhanced surface affinity of the peptide may be a significant factor concerning its function as a fusion promoting agent.

Keywords: Langmuir monolayer; Surface activity; Partitioning equilibrium; Isoelectric point; Capillary electrophoresis; Membrane fusion

1. Introduction

Fusion peptides play an important role in the infection pathway of many enveloped viruses. They induce fusion between the viral envelope and the target cell membrane, thus facilitating that the viral genetic material can enter the cell. The precise fusion mechanism is not known yet. So far several fusion models for these enveloped viruses are discussed in the literature [1–5]. All of them propose similar molecular reaction steps. General features exhibited by all fusion peptides are their markedly hydrophobic character (implying surface activity) and a highly conserved amino acid sequence which comprises in most cases some 10 to 30 amino acids. However, sequence alignments of different fusion peptides have no pronounced homologies. Also, the occasionally promoted idea of so-called sided fusion peptides is not applicable in every case [6]. Furthermore, they are not always located at the terminus of a viral transmembrane protein. Hence the question arises what causes the functionality? To answer this question more structural and thermodynamic information about fusion peptides is needed.

The aim of the present paper is to investigate quantitatively fundamental physico-chemical properties such as the pH-dependent surface activity and the isoelectric point, pI, of the putative fusion peptide of the human immunodeficiency virus type 1 (HIV-1),

* Corresponding author. Fax: +41 61 2672189. E-mail: schwarzg@ubaclu.unibas.ch

PII S0005-2736(97)00029-1

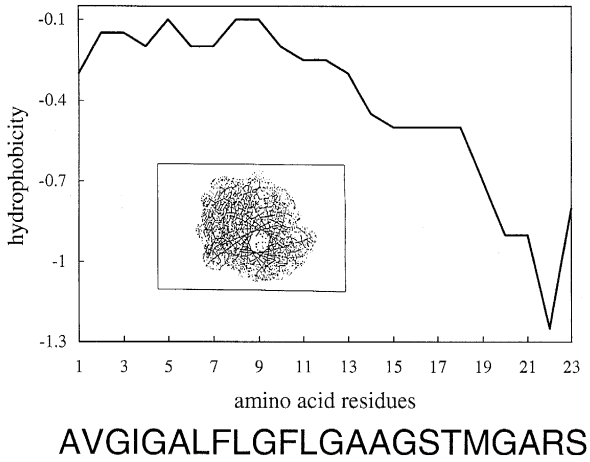

Fig. 1. Sequence of the amino acid residues of the putative HIV-1 gp41-fusion peptide (N → C) and their level of hydrophobicity according to the Chothia scale [9]. The inset presents a 'fried egg' view looking down the backbone of an α-helical conformation with its first hydration shell (dotted area) as calculated by molecular modeling (see text).

representing the 23 amino acid residues at the N-terminus of the viral transmembrane protein gp41. The peptide exerts a well-established surface pressure at an air/water interface [7] and forms an α-helix in trifluoroethanol [8]. The hydrophilic amino acids of the peptide are concentrated at the C-terminus resulting in an amphiphilic structure with a hydrophilic head and a hydrophobic tail analogous to that of a lipid. The amino acid sequence and the distribution of hydrophobicity along the peptide backbone as predicted by the Chothia scale [9] are shown in Fig. 1. When projected in an α-helical conformation the peptide exhibits the shape of a sided fusion peptide with all bulky side chains on one side of the helix ('fried egg' view, see inset of Fig. 1). In a membrane the gp41-fusion peptide is capable of inducing either fusion or lysis, depending on its intramembrane structure being either α-helical or β-sheet [8,10–12]. A possible pH-dependence of the fusion process is still an issue of controversial discussion in the literature [13–15].

2. Theoretical basis

We take advantage of a novel method to process conventional surface activity data of a poorly soluble surfactant so that the partitioning between an air/water interface and the bulk volume becomes accessible quantitatively. This approach is founded on thermodynamic reasoning as described previously in greater detail [16]. Here only its essence will be recapitulated in short.

The starting point is the appropriate mass conservation law

$$n_o = A \cdot \Gamma + V \cdot c_s \tag{1}$$

involving the variables n_o: total amount of spread peptide, A: accessible surface area, Γ: surface concentration (mol per area), V: bulk volume, and c_s: subphase concentration (mol per volume), respectively.

Under equilibrium conditions thermodynamic principles imply that Γ as well as c_s are determined solely by the lateral pressure, π, as an independent variable. Accordingly, a plot of n_o versus A for a fixed pressure at constant V is predicted to result in a straight line. From its slope (Γ) and ordinate intercept ($n_s = V \cdot c_s$) the surface concentration and subphase desorbed amount, respectively, can be readily derived.

We could successfully confirm this linear relationship experimentally with the present HIV-1 gp41-fusion peptide at a subphase pH of 7.5 [16]. In this way Γ and c_s have been evaluated as a function of π. With a view on structural aspects we have then calculated the partial molecular area of the peptide

$$a = (N_A \cdot \Gamma)^{-1} \tag{2}$$

(N_A: Avogadro's number). On the other hand, the relevant Gibbs energy may be expressed in terms of the monolayer-related chemical potential

$$\mu = \mu^{\circ} + RT \cdot \ln(\alpha\Gamma) \tag{3}$$

(μ°: interfacial standard potential) via the pertinent activity coefficient α (reflecting the repulsive peptide-peptide interactions in the monolayer). By means of Gibbs' equation we may numerically calculate this quantity [16] from the measured π and Γ data according to the relation

$$\ln\alpha = \varphi + \int_0^{\Gamma} (\varphi/\Gamma)\,\mathrm{d}\Gamma \quad \textit{where } \varphi = (\pi/\pi_{id}) - 1 \tag{4a}$$

with $\pi_{id} = RT \cdot \Gamma$ (i.e., the surface pressure under the conditions of an ideal 2-dimensional gas). This leads to

$$\Delta G_m = RT \cdot \ln \alpha \quad (4b)$$

standing for the non-ideal contribution to the molar Gibbs energy required to incorporate a peptide molecule into the monolayer at constant area [17].

The course of a as a function of π turned out to exhibit a very substantial decrease that apparently reflects a transition from a larger-area state (presumably an α-helix parallel to the interface) into a smaller-area state (with a more oblique orientation). Having introduced appropriate molecular self-areas (i.e., the Van der Waal's domains), a_o and a (being practically incompressible), the observed average molecular area was expressed as

$$a = x_1 \cdot a_o + x_2 \cdot a \quad (5a)$$

with the corresponding mol fractions x_1 and x_2, respectively. For the smaller-area state we then obtain the expression

$$x_2 = [\Gamma \cdot (\Gamma - \Gamma_o)] / [\Gamma \cdot (\Gamma - \Gamma_o)] \quad (5b)$$

that applies to the range of surface concentrations between $\Gamma_o = 1/(N_A a_o)$ and $\Gamma = 1/(N_A a)$. Below Γ_o only the larger-area (low-pressure) state accordingly exists, whereas above Γ merely the smaller-area (high-pressure) state is encountered. The functional dependence of Γ on c_s or π could then be described by

$$\Gamma = \Gamma_o + [\Gamma_o \cdot e^y \cdot (\Gamma - \Gamma_o)] / [\Gamma + \Gamma_o \cdot e^y] \quad (6)$$

where $y = (\pi - \pi^*)/\pi_o$ or $(c_s - c_s^*)/c_o$, respectively. The characteristic parameters π^*, π_o and c_s^*, c_o were determined on the basis of an experimentally confirmed 'Van 't Hoff' type relationship of the apparent equilibrium constant $K = x_2/x_1$ regarding the applied surface pressure [16].

In the present article this analysis will be extended to a broad range of pH in the neutral and acidic region. The results can be interpreted in terms of pH-sensitive orientational changes that the peptide undergoes in the monolayer. Our findings reveal useful physicochemical properties of the HIV-1 gp41-fusion peptide at a phase boundary between hydrophobic and hydrophilic media, providing possible new insights into the fusion process between the virus and a target cell.

3. Materials and methods

3.1. General technical procedures

The synthesis of gp41-fusion peptide (with a sequence derived from HIV-1 strain LAV_{1a} [7]) and the procedure of the monolayer measurements have been described previously in greater detail [16]. We used a round Teflon trough after Fromherz [18], filled with $V = 48$ ml of buffer. Each compartment was equipped with a tiny Teflon-coated magnetic stirrer. A peptide stock solution (approx. 1 mg/ml) in DMSO (dimethyl sulfoxide, 98% purchased from Fluka, Switzerland) was subsequently spread in small amounts (1 to 5 μl) on the clean air/buffer interface. As demonstrated previously [16] there is no measurable loss of the peptide to the Teflon wall nor does the solvent DMSO influence our monolayer experiments. Performing π versus A-isotherms ('isothermal mode'), measuring at constant π ('isobaric mode') or at constant A ('isochorous mode') under comparable conditions resulted in the same data pairs of n_o and A. Therefore we conclude that our system has reached a thermodynamic equilibrium so that the equations in the theoretical section are applicable. Once equilibrium had been established, π versus A isotherms were recorded with a compression rate of 5 cm^2/min. Measurements always started with very low lateral pressures. They have been performed at room temperature (23 ± 1°C).

The peptide concentrations were determined by performing a periodically repeated quantitative amino acid analysis [16]. Stock solutions have been stored at -18°C in Teflon sealed glass vials under an argon atmosphere.

Molecular modelling of ideal peptide structures was done with the software Insight 2.3 provided by Biosym (San Diego CA, USA).

3.2. Control of pH

Varying the composition of a McIlvaine buffer [19] provided an approximately constant ionic strength (about 60 mM as calculated by an adapted Hender-

son-Hasselbalch equation) over a broad pH range without having to exchange the buffer system. Both buffer components (Na_2HPO_4 and citric acid monohydrat) were purchased from Fluka. The water was processed by a Barnstead NANOpure apparatus (Dubuque, Iowa, USA). The desired pH was adjusted by variation of the buffer components and measured during an individual experiment in the trough with a combined Ag/AgCl flat electrode (Ingold, Urdorf, Switzerland). Control experiments showed no measurable effect of the ions released by the electrode. Calibration and measurement were performed at the same temperature. After each measurement the electrode was treated with water and an acidic pepsin solution to keep it clean.

3.3. Isoelectric focusing

Isoelectric focusing (IEF) was carried out with an Applied Biosystems 270 A high performance capillary electrophoresis (HPCE) system using the ProFocus Kit also supplied from Applied Biosystems (San Jose, CA USA). Measurements were carried out at 30°C with an electric field of 30 kV and the peptide suspended in pure water. The suspension of gp41-fusion peptide in water consists mainly of rod shape aggregates [20]. When using this method the peptide is moved from a pure water environment to a pH gradient by applying an electric field. The movement ceases once the pI is reached. The relative electrophoretic mobility, μ_{rel}, was calculated according to

$$\mu_{rel} = (t_P - t_K)/(t_A - t_K) \quad (7)$$

where t_P is the relative migration time of the peptide sample, t_K and t_A are the relative migration times of the cathode and anode interface [21]. The isoelectric point of the peptide was determined by taking advantage of the linear dependence of μ_{rel} on pI that had been calibrated using 3 reference proteins (RNase A, carbonic anhydrase and CCK flanking peptide). All reagents for isoelectric focusing were prepared freshly before each measurement.

4. Results and discussion

For a series of 15 given pH values ranging from 2.5 up to 7.5 and a constant ionic strength of 60 mM we have determined the specific partitioning data. This includes the results for pH 7.5 adopted from our preceding paper [16]. In Fig. 2 the procedure is demonstrated with data taken at a selected subphase pH of 6.3. Plots of the surface pressure, π, versus the accessible trough area, A, have been registered for a number of different total amounts of peptide, n_o. At a fixed lateral pressure we pick the trough area, A,

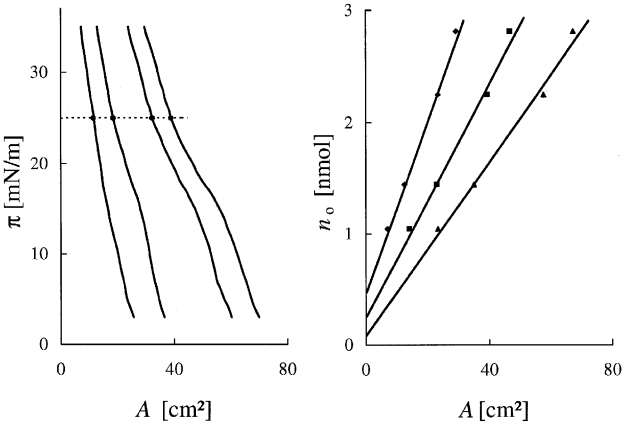

Fig. 2. Processing of original surface activity data measured at pH 6.3. Left panel: Pressure-area isotherms for total amounts of spread peptide $n_o = 1.05$, 1.45, 2.25 and 2.80 nmol (left to right). The intersection points with the dashed line define pairs n_o and A for a fixed surface pressure of 25 mN/m. Right panel: Linear mass conservation plots for $\pi = 5$ (▲), 20 (■) and 35 (◆) mN/m.

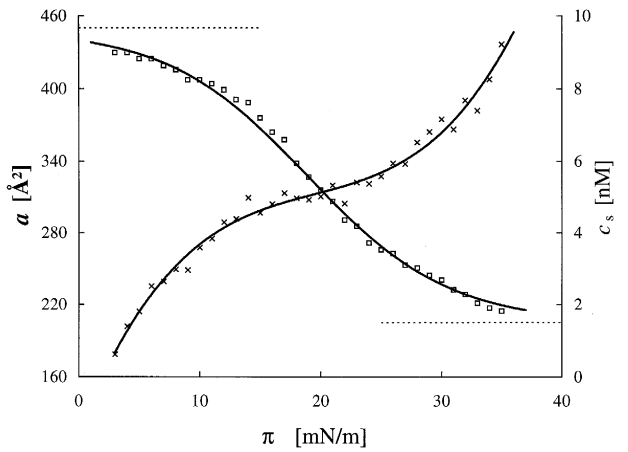

Fig. 3. Plots of the measured partial molecular area, a (□), and the subphase concentration, c_s (×), versus the applied surface pressure for a pH of 6.3. The solid curves have been calculated by means of Eq. (6) with $a_o = 450$ Å^2, $a = 205$ Å^2 (indicated by the dashed line fragments), $\pi^* = 19$ mN/m, $\pi_o = 6.9$ mN/m, $c_s^* = 5.1$ nM, $c_o = 0.9$ nM.

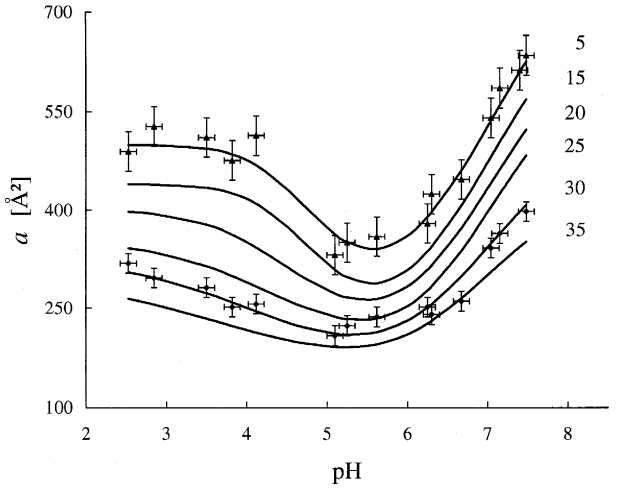

Fig. 4. Variations of the peptide's partial molecular area with pH at selected values of constant pressure (indicated on the right in mN/m). Experimental uncertainties ($\approx \pm 5$–10% for the areas, ± 0.1 for the pH) are displayed by error bars for the examples of 5 and 30 mN/m, respectively.

corresponding to each n_o. According to Eq. (1) the slope of the resulting straight line, n_o versus A, directly measures the surface concentration, Γ, at the given lateral pressure and pH, whereas the ordinate intercept is equal to the subphase amount, $n_s = V \cdot c_s$. In Fig. 3 we present the average partial molecular area, a (calculated with Eq. (2)), and the subphase concentration, c_s, of the peptide in the course of monolayer compression. This reflects a substantial decrease of the peptide's molecular area upon an increasing surface pressure. A transition between two states of different area requirements appears to occur as we had already observed for pH 7.5 [16]. This routine was repeated for any of the pH under consideration.

Table 1
Self-area requirements for ideal secondary structures of gp41-fusion peptide as calculated by molecular modeling

Secondary structure	Area [Å^2]	
	Top view	Side view
α-helix	180	580
β-sheet	80	740
extended	60	830

Top view refers to the area per molecule when the peptide is oriented perpendicular to the interface, side view applies to an orientation parallel to the buffer surface.

Fig. 4 exhibits an overview of the pH dependence that is experienced by the area per peptide molecule at constant π. Assuming that the lowest area per molecule reflects a lack of repulsive electrostatic forces at zero net charge, the apparent minimum area indicates an isoelectric point (pI) of about 5.5 (± 0.5). This is in good agreement with a pI of 6 (± 0.5) resulting from four independent isoelectric focusing measurements carried out in our HPCE apparatus for a fixed concentration where the peptide is supposed to be aggregated [20].

The molecular area characteristics of the monolayer-associated gp41-fusion peptide can be very well described assuming a pressure-induced transition from a larger-area to a smaller-area state. In view of molecular modeling calculations (see Table 1), we propose that at low lateral pressures the peptide assumes the shape of an α-helix lying parallel to the air/water interface, whereas at high values of π it would be compelled to straighten up into a more oblique orientation being in line with our previous conclusion for a neutral pH of 7.5 [16]. Our present study shows that this phenomenon undergoes a pronounced quantitative modification when the pH in the subphase is reduced.

For any special pH under consideration we have evaluated the characteristic parameters that were introduced in the context of Eq. (5a), Eq. (5b) and Eq. (6). The two individual self-areas, a_o and a , as well

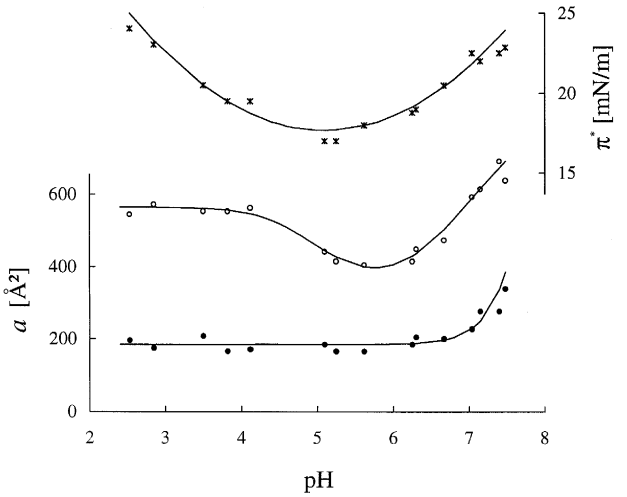

Fig. 5. The pH effect on the molecular self-areas, a_o (○) and a (●), in the low- and high-pressure interfacial states. Also the halfway pressure π^* (×) is shown (see text).

Table 2
Fit parameters used for the measured pH values

pH	7.5	7.4	7.2	7.0	6.7	6.3	6.2	5.6	5.3	5.1	4.1	3.8	3.5	2.9	2.5
π^* [mN/m]	22.9	22.5	22.0	22.5	20.5	19.0	18.8	18.0	17.0	17.0	19.5	19.5	20.5	23.0	24.0
π_o [mN/m]	5.3	6.0	7.0	7.8	7.5	6.9	8.0	9.0	10.0	8.0	7.5	8.5	8.0	8.5	10.0
c_s^* [nM]	5.7	5.0	8.7	7.0	1.5	5.1	5.0	8.0	10.0	18.0	3.6	5.0	2.0	5.1	9.8
c_o [nM]	0.9	0.8	1.4	0.6	1.0	0.9	2.5	2.9	4	4.5	1.0	1.1	0.5	1.7	1.4

as the halfway pressure π^* (where $x_2 = 0.5$, corresponding to 50% orientational turn-over) are presented in Fig. 5. The additional quantities π_o, c_s^* (halfway concentration in the subphase) and c_o are collected in Table 2. We can so very well fit all our measured a (or alternatively Γ) and c_s as a function of π (as for example shown in Fig. 3 for pH 6.3). Furthermore, we may calculate Γ as it depends on c_s (representing the partitioning isotherm between the monolayer and bulk volume phases).

From a thermodynamic point of view we direct our attention to the work that must be done in order to squeeze a peptide molecule into an already existing monolayer. This is expressed as the Gibbs energy ΔG_m introduced by Eq. (4a) and Eq. (4b). We have calculated it from our Γ vs. π data. In Fig. 6 the results are plotted as a function of Γ for the special case of pH 6.3. At the apparent threshold value $\Gamma = 36.9$ pmol/cm^2 (being equal to the corresponding Γ_o) the appropriate insertion energy undergoes an abrupt increase reflecting the onset of strong intermolecular repulsion forces. These are presumably caused by a close encounter of the self-areas. The system will then tend to diminish the implied strain by turning into a state of less area requirement that eventually reduces the steep increment of ΔG_m at more crowding of the molecules. Fig. 6 also features the insertion energy as it is modified upon a change of the pH. Again we note a minimum which can be readily attributed to a lack of repulsive electrostatic forces in the case of the suspected isoelectric point.

The thus indicated pI of 5.5 (± 0.5) stands in an obvious contrast to the value of 10.1 which is predicted on the basis of the aqueous pK-values of the

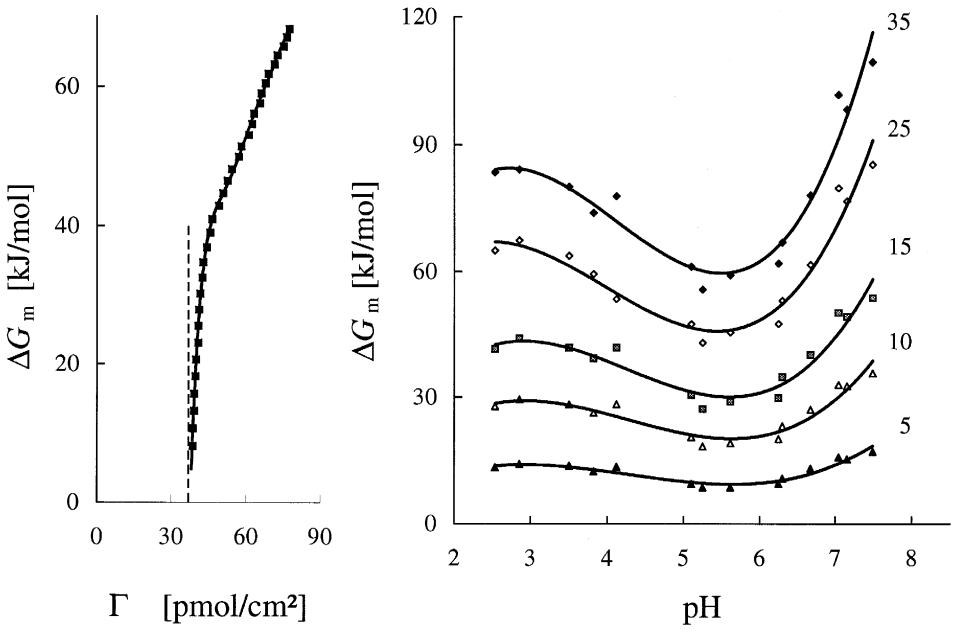

Fig. 6. The molar Gibbs energy of peptide incorporation into the monolayer according to the Eqs. (4a) and (4b) (see text). Left panel: Data for pH 6.3 regarding the impact of repulsive forces when the surface concentration exceeds a threshold value Γ_o. Right panel: Effect of pH at a number of constant lateral pressures (indicated in mN/m on the right).

relevant amino acid residues (i.e., 12.5 for Arg^+ at position 22, in addition to 7.8 and 3.8 for the N- and C-terminal groups, respectively). We must, however, take into account that the surroundings of the charged groups is substantially changed under the present conditions. In the monolayer the molecules are packed closely together at the interface. The same should be true for our IEF experiments where the peptide forms rod-shaped micelles [20]. The apparent drop of the pI could be explained by the change of the physical environment of the peptide molecule at a boundary between a relatively high dielectric constant (water) and a domain with a low dielectric constant (air or the hydrophobic core of the micelles, respectively). The observed $\Delta\mathrm{pK} = -4.6$ can actually be rationalized by an increase of the standard Gibbs energy $\Delta G^{\varnothing}$ that is due to the higher Born self-energies of the NH_3^+ located at the N-terminal alanine and the arginine residue at position 22. This leads to

$$\Delta G^{\varnothing} = \Delta G_{\mathrm{o}}^{\varnothing} + \left[\left(N_{\mathrm{A}} e_0^2\right)/(8\pi\epsilon_{\mathrm{v}} R_{\mathrm{i}})\right]\left[\epsilon^{-1} - \epsilon_0^{-1}\right] \tag{8}$$

for one elementary charge e_0 on a group having a radius R_{i} in an environment with the dielectric constant ϵ (ϵ_{v} stands for the permitivity of vacuum). $\Delta G_{\mathrm{o}}^{\varnothing}$ refers to an environment with the dielectric constant ϵ_0 (water). By assuming an ion radius of 5 Å and a physically reasonable ϵ of 5, one actually arrives at a decrease of each of the two basic pK by 4.6 units. The effect of other ionic species in the surface domain is neglected since these should be forced off into the favorable dielectric medium of the aqueous subphase. A similar pK shift of 2 units to more acidic values was observed in the case of air/water monolayers of substance P, a peptide with the biological function of a neurotransmitter [22].

It should be noted, however, that according to Fig. 5 the smaller self-area is not affected in the acidic pH-range. This suggests a different charge structure of the two orientational states. Naturally the N-terminal amino group of the hydrophobic part would be pushed farther off the water surface into the dielectric domain of the air. Presumably this lowers the pK even more than in the flat position so that there is no N-terminal charge at all under the given circumstances. On the other hand, a zwitterionic configuration is built up at the hydrophilic end which dips into the aqueous medium. Then appreciable electrostatic repulsion resulting in an increase of a is to be expected only at higher pH where merely the negative charge of the C-terminal carboxyl group has survived.

The surface concentration of the gp41-fusion peptide (derived by inverting Eq. (2)) for a fixed surface pressure has its uppermost value (e.g., about 83 pmol/cm^2 at 35 mN/m, which corresponds to an area per molecule of about 200 $Å^2$) at pH 5.5, while the halfway pressure π^* assumes a minimum value (see Fig. 5). At this pH the molecules can obviously pack most closely because they are forced to straighten up by the applied pressure. In other words, when approaching the pI, the hydrophilic/lipophilic balance, HLB, of the gp41-fusion peptide is shifted to a more lipophilic value, thus improving its potential to penetrate a lipid phase.

The partitioning isotherms (i.e., Γ versus c_{s}) exhibit some kind of saturation at higher pressures indicating an equilibrium pressure above which all additional peptides would be pushed into the subphase as reported by the group of DeGrado [7]. Some of our experiments (data not shown) suggest, however, that at pressures above approx. 35 mN/m (depending on pH) the partitioning isotherm appears to raise again. Possibly there is another transition, leading perhaps to a β-sheet conformation. Although quantification in that region suffers from a greater uncertainty, we nevertheless observe a clear trend towards a transition to an even lesser area-requiring state.

The fusion process being presumably mediated by the peptide sequence under consideration is a multistep operation whose molecular details are still unclear. Our experiments show that the peptide's affinity to a hydrophobic interface would be favored by an aqueous pH of about 5.5. In the case of the native gp41 protein there is of course no negative charge at position 23 (i.e., the C-terminal end of the present peptide). It remains, however, the apparent disappearance of the N-terminal positive charge for a sufficiently low pH (owing to the reduced pK of some 3.2). Accordingly physiogenic activity should be promoted in an acidic environment because of the implied advantage regarding penetration into the membrane of a target cell. In order to explore that aspect

more directly, we have started pertinent studies probing the peptide when it actually interacts with a lipid monolayer [23].

Acknowledgements

This research has been supported by Grants 31-042045.94 and 21-045433.95 of the Swiss National Science Foundation. We are grateful to Ch. Stürzinger for his assistance in the HPCE work, to Dr. Gerhard Wackerbauer for helpful discussions and to Dr. Vincent Ball for his thorough proof-reading of this article.

References

[1] F.W. Tse, A. Iwata, W. Almers, J. Cell Biol. 121 (1993) 543–552.
[2] D.P. Siegel, in: J. Bentz (Ed.), Viral Fusion Mechanisms, CRC Press, Boca Raton, 1992.
[3] J. Bentz, H. Ellens, D. Alford, in: J. Bentz (Ed.), Viral Fusion Mechanisms, CRC Press, Boca Raton, 1993, pp. 163–199.
[4] T. Stegmann, J.M. Delfino, F.M. Richards, A. Helenius, J. Biol. Chem. 266 (1991) 18404–18410.
[5] A. Colotto, I. Martin, J.-M. Ruysschaert, A. Sen, S.W. Hui, R.M. Epand, Biochemistry 35 (1996) 980–989.
[6] W.R. Gallaher, J.P. Segrest, E. Hunter, Cell 70 (1992) 531–532.
[7] M. Rafalski, J.D. Lear, W.F. DeGrado, Biochemistry 29 (1990) 7917–7922.
[8] L.M. Gordon, C.C. Curtain, Y.C. Zhong, A. Kirkpatrick, P.W. Mobley, A.J. Waring, Biochim. Biophys. Acta 1139 (1992) 257–274.
[9] C. Chothia, J. Mol. Biol. 105 (1976) 1–14.
[10] I. Martin, M.-C. Dubois, F. Defrise-Quertain, T. Saermark, A. Burny, R. Brasseur, J.-M. Ruysschaert, J. Virol. 68 (1995) 1139–1148.
[11] P.W. Mobley, C.C. Curtain, A. Kirkpatrick, M. Rostamkhani, A.J. Waring, L.M. Gordon, Biochim. Biophys. Acta 1139 (1992) 251–256.
[12] J.L. Nieva, S. Nir, A. Muga, F.M. Goñi, J. Wiltschut, Biochemistry 33 (1994) 3201–3209.
[13] Y.N. Vaishnav, F. Wong-Staal, Annu. Rev. Biochem. 60 (1991) 577–630.
[14] C. Larsen, H. Ellens, J. Bentz, in: R.C. Aloia, C.C. Curtain, L.M. Gordon (Eds.), Advances in Membrane Fluidity 6, Wiley-Liss, New York, 1992, pp. 1–25.
[15] V.A. Slepushkin, G.B. Melikyan, M.S. Sidorova, V.M. Chumakov, S.M. Andreev, R.A. Manulyan, E.V. Karamov, Biochem. Biophys. Res. Commun. 172 (1990) 952–957.
[16] G. Schwarz, S.E. Taylor, Langmuir 11 (1995) 4341–4346.
[17] G. Wackerbauer, I. Weis, G. Schwarz, Biophys. J. 71 (1996) 1422–1427.
[18] P. Fromherz, Rev. Sci. Instr. 46 (1975) 1380–1385.
[19] T.C.J. McIlvaine, J. Biol. Chem. 49 (1921) 183–187.
[20] V.A. Slepushkin, G.V. Kornilaeva, S.M. Andreev, M.V. Sidorova, A.O. Petrukhina, G.R. Matsevich, S.V. Raduk, V.B. Grigoriev, T.V. Makarova, V.V. Lukashov, E.V. Karamov, Virology 194 (1993) 294–301.
[21] S.E. Moring, J.C. Colburn, P.D. Grossman, H.H. Lauer, LC GC 8 (1990) 34–36.
[22] A. Seelig, Biochim. Biophys. Acta 1030 (1990) 111–118.
[23] G. Schwarz, S.E. Taylor, Supramol. Sci., 1996, in press.